

## Theoretical and Experimental Investigation of the Dynamical Behaviour of Complex Configuration Rotors

Prof. Mohsin Juber Jweeg  
Dep. of Mechanical Eng.  
College of Engineering  
Alnhain University

Lect. Mahmud Rasheed Ismail  
Dep. of Mechanical Eng.  
College of Engineering  
Alnhain University  
Email: mahmech2001@yahoo.com

Zainab Mohammed Hwady  
Dep. of Mechanical Eng.  
College of Engineering  
Alnhain University

### ABSTRACT:

The present work considers an alternative solution for a complex configuration of rotor discs by applying Galerkin Method. The theoretical model consists of elastic shaft carrying number of discs and supported on number of journal bearings. The equation of motion was discretized to finite degree of freedom in terms of the system generalized coordinates. The various effects of the dynamical forces and moments arising from the bearing, discs and shaft were included. Rayleigh beam model is used for analyzing the shaft while the discs are considered rigid. The validity and convergence of the present analysis was carefully checked by comparing with the Finite Element solution. An example of rotor consists of three different size discs and supported by two journal bearing was considered for the numerical solution. The results shows good agreements between the two methods, where the maximum error not exceeds 5%. The convergence test showed that using few modes (not more than 6) are sufficient for the accurate analysis. The forward and backward whirl was investigated experimentally. The experimental results of a two discs rotor, show a reasonable agreement where the maximum error not exceeds 11%. The unbalance response, Campbell diagram, orbit response were plotted. The effects of geometry, disc sizes, location and arrangement on the unbalance response and natural frequencies of three discs rotor were further investigated.

**Key words:** Galerkin method, Campbell diagram, whirl frequency, journal bearing, gyroscopic couple

### مبحث نظري وتجريبي للتصرفات الديناميكية لدوارات معقدة الاشكال

زينب محمد هويدي  
قسم الهندسة الميكانيكية  
كلية الهندسة / جامعة النهريين

م. محمود رشيد اسماعيل  
قسم الهندسة الميكانيكية  
كلية الهندسة / جامعة النهريين

أ.د. محسن جبر جويج  
قسم الهندسة الميكانيكية  
كلية الهندسة / جامعة النهريين

### الخلاصة:

تم في البحث الحالي اعتماد طريقه بديلة لتحليل الدوار المعقد، وذلك باستخدام طريقة جالركين. يتألف النموذج النظري من عمود مرن يحمل عدد من الاقراص والمسند الزيتيه. تم نجزئة معادلة الحركة الى عدد محدد من درجات الحرية باستخدام الاحداثيات العامة. تم الاخذ بنظر الاعتبار التأثيرات الديناميكية للقوى والعزوم الناتجة من تأثيرات المساند الاقراص وعمود الدوران. تم اعتبار العمود كعمود رايلي اما الاقراص فاعتبرت كتل صلدة. اختبرت صحة وتقارب الحل بالمقارنة مع طريقة العناصر المحدده FEM. وكمثال عددي تم اختيار دوار مؤلف من عمود يحمل ثلاثة اقراص مختلفة الحجم ومسند على مسندين زيتيين. بينت النتائج تطابق جيد بين الطريقتين حيث لم تتعدى نسبة الخطأ 5% بينما بينت تجربة اقتراب الحل بان استخدام عدد قليل من الاطوار (لا يتعدى 6) يكفي للحصول على نتائج جيدة. بعض الخصائص الديناميكية مثل تردد التدويم الامامي والخلفي تم قياسها عمليا باستخدام نموذج لدوار مؤلف من قرصين، فبينت النتائج تطابق مقبولا حيث لم تتعدى نسبة الخطأ 11%. تم رسم مخططات استجابة عدم الاتزان ومخطط كامبل وشكل المدارات لنماذج من الدوارات. بالاضافة الى ذلك، فقد تم دراسة تأثير حجم وترتيب وموقع الاقراص على الاستجابة والترددات الطبيعيه لدوار مؤلف من ثلاثة دسكات.

الكلمات الرئيسية: طريقة جالركين، مخطط كامبل، تردد التدويم، مسند زيتي، العزم الجايروسكوبي

## 1. INTRODUCTION

Rotors and rotary machines have a significant application in engineering and industries. Many catastrophic damages of machines are due to the undesired dynamical behavior of the rotors, such as; whirling and large deflection, resonance, imbalance shaking forces,...etc.

In 1869, the first attempt to formulate the dynamics of single disc rotor had been put forward by Rankin. However the first simplified acceptable model had been proposed by Jeffcott in 1919. From that time till now, enormous theoretical and experimental works had been achieved in this vast field, hence, rotor-dynamics bibliography is much extended. A comprehensive survey about this subject can be found in many references such as **Genta,2005**.

The main kinds of effects contribute the dynamical behavior of rotors; The elasticity ,inertia and gyroscopic effects of the shaft , the elasticity and damping of the oil film at bearings, and the gyroscopic ,inertial (lateral and rotational) and unbalance of the attached discs. Including all these effects, will complicate the analysis even for the simplest models, **Holmes,1978**. The dynamical analysis of multi disc and bearings rotors were normally achieved via numerical methods such as Finite Element, influence coefficients ,state space ,lumped analysis and transfer matrix method. For example, **Geradin,1984**, introduced a new Finite element model for evaluating the natural frequencies and dynamics response of multi disc rotos .**Rao ,1994**, used the Influence coefficient method to calculate the natural frequencies of multi disc rotor . **Das and Dutt,2012**, employed state space method to evaluate the vibration of multi disc rotors for controlling process .

The effect of the unbalancing of multi disc rotor on the dynamical behavior and stability was studied by **Ding ,1997 and Xie .et.al 2008** .They used the lumped mass method for the analysis. For all of the above mentioned methods ,the accurate analysis demand four degree of freedom for the individual station (two translations and two rotations).Hence large number of stations are needed for accurate numerical analysis. This lead to a huge global matrix for analyzing the Eigen value problem and frequency response. Analytical methods are seldom used except for simple or high approximated models, **Adams,2010**.Many experimental works was performed to justify the

theoretical investigation of multi disc rotors .For example ,**Flack, et.al ,1981**, conducted experiment to investigate the effect of lubricant viscosity on the response of three mass rotor . **Ding, et al.,2005**, made experimental study to predict the nonlinear dynamic behaviors of a multi-bearing flexible rotor system.

In the present work, An alternative method for evaluating the dynamical behavior of multi discs and bearings rotor will be attempted . In this method , Galerkin procedure is employed, in which an appropriate shape functions are selected as basis functions for performing the analysis . Such functions take into account the elastic deformation of the shaft as well as the possibility of rigid body translation and rotation.

## 2. THEORY

For the multi discs and bearings model shown in **Fig.1**, the flexible shaft was considered to obey Rayleigh beam, and subjected to bending vibration at two orthogonal planes  $x-z$  and  $x-y$ . The various forces and moments due to the stiffness and damping of the bearing oil film, disc inertia, rotary inertia, gyroscopic and unbalancing for the rotor components, are shown in **Fig.2**.

The equations of motion of bending vibration can be written as, **Ding,2005**:

$$EI \frac{\partial^4 w}{\partial x^4} + \rho A \frac{\partial^2 w}{\partial t^2} + C \frac{\partial w}{\partial t} - \rho I \frac{\partial^2}{\partial x^2} \left( \frac{\partial^2 w}{\partial t^2} \right) - 2\rho I \omega_{sp} \frac{\partial^2}{\partial x^2} \left( \frac{\partial v}{\partial t} \right) = f_z(x,t) \quad (1)$$

$$EI \frac{\partial^4 v}{\partial x^4} + \rho A \frac{\partial^2 v}{\partial t^2} + C \frac{\partial v}{\partial t} - \rho I \frac{\partial^2}{\partial x^2} \left( \frac{\partial^2 v}{\partial t^2} \right) + 2\rho I \omega_{sp} \frac{\partial^2}{\partial x^2} \left( \frac{\partial w}{\partial t} \right) = f_y(x,t) \quad (2)$$

Dividing Eq. (1) and Eq. (2) by  $EI$  and arranging, giving:

$$\eta^{IV} + \dot{\eta} + C^* \dot{\eta} - \beta \ddot{\eta}'' - 2\beta \Omega \dot{\mu}'' = \alpha \cdot f_z(\zeta, \tau) = Q_z(\zeta, \tau)$$

$$\mu^{IV} + \dot{\mu} + C^* \dot{\mu} - \beta \ddot{\mu}'' + 2\beta \Omega \dot{\eta}'' = \alpha \cdot f_y(\zeta, \tau) = Q_y(\zeta, \tau) \quad (3)$$

Where;

$$\eta = w/L, \quad \mu = v/L, \quad \zeta = x/L,$$

$$\tau = (t/L^2) \sqrt{EI/\rho A}, \quad \Omega = \omega_{sp} L^2 \sqrt{\rho A/EI}$$

$$\beta = I/L^2 A, \quad C^* = \frac{CL}{\sqrt{EI\rho A}}, \quad \alpha = L^3/EI \quad (4)$$

For simplicity the following notations were used;

$$\frac{\partial}{\partial \tau}(\ ) = (\ ) \cdot \quad \text{And} \quad \frac{\partial}{\partial \zeta}(\ ) = (\ )'$$

The R.H.S terms of Eq.(3) represents the dimensionless dynamical forces due to the bearing and discs at x-z and x-y planes. In case of,  $Q_z$  they are as follows;

1-bearing spring forces;

$$F_{SZ} = \frac{-\alpha}{L} \sum_{i=1}^{Nb} K_{iz} w(x, t) = - \sum_{i=1}^{Nb} K_{iz}^* \eta \tag{5}$$

2- bearing damping forces;

$$F_{DZ} = \frac{-\alpha}{L} \sum_{i=1}^{Nb} C_{iz} \frac{\partial w}{\partial t} = - \sum_{i=1}^{Nb} C_{iz}^* \dot{\eta} \tag{6}$$

2- Disc translation inertial forces:

$$F_{TZ} = \frac{-\alpha}{L} \sum_{j=1}^{Nd} m_j \frac{\partial^2 w}{\partial t^2} = - \sum_{j=1}^{Nd} m_j^* \ddot{\eta} \tag{7}$$

3- Disc imbalances forces;

$$F_{bz} = \frac{\alpha}{L} \sum_{j=1}^{Nd} m b_j e \omega_{sp}^2 \sin \omega_{sp} t = \sum_{j=1}^{Nd} m b_j^* e^* \Omega^2 \sin \Omega \tau \tag{8}$$

4-Disk gyroscopic moments;

$$M_{GZ} = -\frac{\alpha}{L} \sum_{j=1}^{Nd} J_j \omega_{sp} \frac{\partial}{\partial t} \left( \frac{\partial v}{\partial x} \right) = \sum_{j=1}^{Nd} J_j^* \Omega \dot{\mu}' \tag{9}$$

5-Disc rotational inertia moments;

$$M_{RZ} = \frac{-\alpha}{L} \sum_{j=1}^{Nd} J_j \frac{\partial^2}{\partial t^2} \left( \frac{\partial w}{\partial x} \right) = - \sum_{j=1}^{Nd} J_j^* \ddot{\eta}' \tag{10}$$

Where  $N_b$  and  $N_d$  are the number of bearings and discs, respectively .

For the plan x-y the same procedures can be used to obtain the components of the force  $Q_y$  as the follows:

$$F_{SY} = - \sum_{i=1}^{Nb} K_{iy}^* \mu \tag{11}$$

$$F_{DY} = - \sum_{i=1}^{Nb} C_{iy}^* \dot{\mu} \tag{12}$$

$$F_{TY} = - \sum_{j=1}^{Nd} m_j^* \ddot{\mu} \tag{13}$$

$$F_{bY} = \sum_{j=1}^{Nd} m b_j^* e^* \Omega^2 \sin \Omega \tau \tag{14}$$

$$M_{GY} = \sum_{j=1}^{Nd} J_j^* \Omega \dot{\eta}' \tag{15}$$

$$M_{RY} = - \sum_{j=1}^{Nd} J_j^* \ddot{\eta}' \tag{16}$$

In the above equations, the following dimensionless terms are considered;

$$\begin{aligned} K_{iz}^* &= \frac{K_{iz} L^3}{EI}, \quad K_{iy}^* = \frac{K_{iy} L^3}{EI} \\ C_{iy}^* &= \frac{C_{iy}}{\sqrt{\rho A E I}}, \quad C_{iz}^* = \frac{C_{iz}}{\sqrt{\rho A E I}} \\ J_j^* &= \frac{J_j}{\rho A L^3}, \quad m_{b_j}^* = \frac{m b_j}{\rho A L}, \quad m_j^* = \frac{m_j}{\rho A L} \\ e^* &= \frac{e}{L} \end{aligned} \tag{17}$$

Substituting Eqs.(5 to 10) into the first of Eq.(3) giving the following equation of motion at (x-y) plane;

$$\begin{aligned} \eta'''' + \dot{\eta} + \bar{C} \dot{\eta} - \beta \eta'' - 2\beta \Omega \mu'' \\ + \sum_{i=1}^{Nb} \bar{K}_{iz} \eta + \sum_{i=1}^{Nb} C_{iz}^* \dot{\eta} + \sum_{j=1}^{Nd} m_j^* \ddot{\eta} - \sum J_j^* \Omega \dot{\mu}' \\ + \sum_{j=1}^{Nd} J_j^* \ddot{\mu}'' = \sum_{j=1}^{Nd} m b_j^* e^* \Omega^2 \sin \Omega \tau \end{aligned} \tag{18}$$

Similarly ,substituting Eqs.(11-16),into the second of Eqs.(3) giving the equation of motion at (x-z) plane;

$$\begin{aligned} \mu'''' + \ddot{\mu} + C^* \dot{\mu} - \beta \ddot{\mu}'' + 2\beta \Omega \dot{\eta}'' \\ + \sum_{i=1}^{Nb} K_{iy}^* \mu + \sum_{i=1}^{Nb} C_{iy}^* \dot{\mu} + \sum_{j=1}^{Nd} m_j^* \ddot{\mu} - \sum_{j=1}^{Nd} J_j^* \Omega \dot{\eta}' \\ + \sum_{j=1}^{Nd} J_j^* \ddot{\mu}'' = \sum_{j=1}^{Nd} m b_j^* e^* \Omega^2 \sin \Omega \tau \end{aligned} \tag{19}$$

To introduce Galerkin scheme ,a solution in term of the beam normal modes may be taken . Let such solutions of eqs(18) and (19) be:

$$\eta(\zeta, \tau) = \sum_{s=1}^N \phi_s(\zeta) q_s(\tau) + \phi_T(\zeta) q_T(\tau) + \phi_R(\zeta) q_R(\tau)$$

$$\mu(\zeta, \tau) = \sum_{s=1}^N \psi_s(\zeta) p_s(\tau) + \psi_T(\zeta) p_T(\tau) + \psi_R(\zeta) p_R(\tau) \quad (20)$$

In eqs.(20);  $\phi_s(\zeta)$  and  $\varphi_s(\zeta)$  stand for the normal modes of beam free vibration,  $\phi_T$  and  $\varphi_T$  for translational modes and  $\phi_R$ ,  $\varphi_R$  for rotational modes in z and y directions, respectively. In the absence of all the forces and moments the normalized mode shapes  $\phi_s(\zeta)$  and  $\varphi_s(\zeta)$  are those of free-free beam which take the following form, **Lund et al.,1978:**

$$\phi_s(\zeta) = \varphi_s(\zeta) = \sin \lambda_s \zeta + \sinh \lambda_s \zeta - \sigma_s (\cos \lambda_s \zeta + \cosh \lambda_s \zeta) \quad (21)$$

Where;

$$\sigma_s = \frac{\sinh \lambda_s - \sin \lambda_s}{\cosh \lambda_s - \cos \lambda_s}, \text{ and}$$

$\lambda_s$  are the Eigen values of the free-free beam.

The normalized modes of translational and rotational modes may be taken as;

$$\phi_T(\zeta) = \psi_T(\zeta) = 1$$

$$\phi_R(\zeta) = \psi_R(\zeta) = \zeta$$

So that **Eq (20)** become;

$$\eta(\zeta, \tau) = \sum_{s=1}^N \phi_s(\zeta) q_s(\tau) + q_T(\tau) + \zeta q_R(\tau) \quad (22)$$

$$\mu(\zeta, \tau) = \sum_{s=1}^N \psi_s(\zeta) p_s(\tau) + p_T(\tau) + \zeta p_R(\tau) \quad (23)$$

Substitute **Eq. (22)** into **Eq. (18)**, and following Galrkin procedure in which another series for the

r modes is chosen as :

$$\phi_r(\zeta) = \sum_{r=1}^N \phi_r(\zeta) + 1 + \zeta$$

Now , multiply , integrate from 0 to 1 and make use of the orthogonally of the normal modes, the following matrix equation can be obtained as;

$$[A]\{\dot{q}\} + [B]\{\ddot{q}\} + C^*[B]\{\dot{q}\} - \beta[S]\{\ddot{q}\} - 2\beta\Omega[s]\{\dot{p}\} + \sum_{i=1}^{Nb} (K_{iz}^*[H_i]\{\dot{q}\} + C_{iz}^*[H_i]\{\ddot{q}\}) + \sum_{j=1}^{Nd} (m_j^*[T_j]\{\dot{q}\} + J_j^*[V_j]\{\ddot{q}\} - J_j^*\Omega[V_j]\{\dot{p}\}) = \sum_{j=1}^{Nd} mb_j^* e^* \Omega^2 \cos \Omega \tau [W_j] \quad (24)$$

By the similar procedures one can obtain from eq.(23) and (19) the following matrix equation;

$$[A]\{\dot{p}\} + [B]\{\ddot{p}\} + C^*[B]\{\dot{p}\} - \beta[S]\{\ddot{p}\} + 2\beta\Omega[s]\{\dot{q}\} + \sum_{i=1}^{Nb} (K_{iy}^*[H_i]\{\dot{p}\} + C_{iy}^*[H_i]\{\ddot{p}\}) + \sum_{j=1}^{Nd} (m_j^*[T_j]\{\dot{p}\} + J_j^*[V_j]\{\ddot{p}\} + J_j^*\Omega[V_j]\{\dot{q}\}) = \sum_{j=1}^{Nd} mb_j^* e^* \Omega^2 \sin \Omega \tau [W_j] \quad (25)$$

The elements of the matrices  $[A]$  , $[B]$  , $[S]$  , $[H_i]$  , $[T_j]$  , $[V_j]$  , $[W_j]$  are given in the appendix.

Finally, **Eqs. (24) and (25)** can be arranged in the following standard form;

$$[K_z]\{\dot{q}\} + [C_z]\{\ddot{q}\} - \Omega[G]\{\dot{p}\} + [M]\{\ddot{q}\} = \{W\} \cos \Omega \tau \quad (26)$$

$$[K_y]\{\dot{p}\} + [C_y]\{\ddot{p}\} + \Omega[G]\{\dot{q}\} + [M]\{\ddot{p}\} = \{W\} \sin \Omega \tau \quad (27)$$

Where;

$$[K_z] = [A] + \sum_{i=1}^{Nb} (K_{iz}^*[H_i])$$

$$[K_y] = [A] + \sum_{i=1}^{Nb} (K_{iy}^*[H_i])$$

$$[C_z] = C^*[B] + \sum_{i=1}^{Nb} (C_{iz}^*[H_i])$$

$$[C_y] = C^*[B] + \sum_{i=1}^{Nb} (C_{iy}^*[H_i])$$

$$[G] = 2\beta[S] + \sum_{j=1}^{Nd} J_j^*[V_j], \text{ and}$$

$$[M] = [B] - \beta[S] + \sum_{j=1}^{Nd} m_j^*[T_j] + J_j^*[V_j]$$

$$\{W\} = \sum_{j=1}^{Nd} mb_j^* e^{*} \Omega^2 [W_j] \quad (28)$$

**2.1 Unbalance response and critical speeds**

Eqs.(26) and (27) can be arranged in a single equation by using the following complex vector;

$$\{u\} = \{q\} + i\{p\} \quad (29)$$

Now ,multiplying Eq.( 26) by i ( $i = \sqrt{-1}$ ), adding to Eq.(25) and applying Eq.(29) will give;

$$[K]\{u\} + [C]\{\dot{u}\} + i\Omega[G][I]\{\dot{u}\} + [M][I]\{\ddot{u}\} = \{W\}e^{i\Omega t} \quad (30)$$

Where;

$$[K] = \begin{bmatrix} K_z & 0 \\ 0 & K_y \end{bmatrix}, \quad [C] = \begin{bmatrix} C_z & 0 \\ 0 & C_y \end{bmatrix}, \quad [I] = \begin{bmatrix} 1 & 0 \\ 0 & 1 \end{bmatrix} \quad (31)$$

Since the imbalanced force is harmonic, the steady state response of Eq.(30) can be written as;

$$\{u\} = \left[ [K] + i\Omega[C] + i\Omega[G][I] - \Omega^2[M][I] \right]^{-1} \{W\}e^{i\Omega t} \quad (32)$$

Eq.(32) as well as Eqs.(22) and (23) can be used for calculating and plotting the response due to unbalancing at a given range of spin speeds .The speeds which give the maximum amplitude are the critical speeds. The effect of any parameter related to the rotor configuration can be studied by using this equation.

It is important to note that; the present analysis assumes the unbalance vectors lie in the same planes for all discs .However for the case when there is different unbalance planes of discs ,a spatial consideration for solving Eq.(32) must be made .This case is not dealt in the present analysis

**2.1 Campbell Diagram**

The forward and backward whirling frequencies at a given spin speed can be calculated by using the homogenous parts of Eqs. (26) and (27) which are;

$$[K_z]\{q\} + [C_z]\{\dot{q}\} - \Omega[G]\{\dot{p}\} + [M]\{\ddot{q}\} = 0 \quad (33)$$

$$[K_y]\{p\} + [C_y]\{\dot{p}\} + \Omega[G]\{\dot{q}\} + [M]\{\ddot{p}\} = 0 \quad (34)$$

Since vibration is harmonic motion, one can assume the following solutions for q and p;

$$\{q\} = \{\hat{q}\}e^{i\omega t}, \{p\} = \{\hat{p}\}e^{i\omega t} \quad (35)$$

Where  $\{\hat{q}\}, \{\hat{p}\}$  are arbitrary constants .

Substituting Eq. (35) into Eqs. (33) and (34) and eliminating the arbitrary constants yield to the following characteristics determinant;

$$\begin{vmatrix} [K_z] + i\omega[C_z] - \omega^2[M] & -i\omega\Omega[G] \\ i\omega\Omega[G] & [K_y] + i\omega[C_y] - \omega^2[M] \end{vmatrix} = 0 \quad (36)$$

At a given rotor parameters Eq.(36) can be used to construct campbell diagram .by plotting the backward and forward frequencies for selected modes against the spin speeds .

**2.3 Finite element solution**

For Finite element analysis ,ANSYS 14 software was employed . Three element types are selected to define the various rotor components which are; MASS21 element for discs, BEAM 188 element for shaft and COMBI214 element for Bearings.

The shaft is divided to 32 elements .The gyroscopic effect was considered by employing the rotating axis via the CORIOLIS and OMEGA commands .The HARMONIC ANALYSIS is used for evaluating the solution and plotting the results.

**3-EXPERIMENTAL INVESTIGATION**

The aim of the experimental work is carried to verify the present theoretical analysis. For this purpose, a model of rotor consisted of a two different size brass discs fitted on elastic steel shaft and sited on two identical journal bearings as shown in Fig.3-a was used. The specifications of the model are given in table(1) except that disc(1) was excluded .Disc(2) and (3) were located at 0.35 and 0.25m from the shaft right side end .The rotor is driven by an electrical motor with variable speed of (0-3000) RPM .In order to investigate the forward and backward whirl frequencies ,the motor has a facility of changing its speed directions .To reduce the undesired effect of the motor vibration which may interfere with the rotor response, a PVC coupling was used. A special attention was made for aligning the shaft with the

motor shaft and the bearings to insure center to center alignment which is necessary for reducing the misalignment effect on the response. A special mechanism was introduced to measure the response of the rotating shaft, since it is impossible to fit a pick up device directly on the rotating shaft. This mechanism consists of a small light rod slides vertically through a slot in the supported frame. A soft spring is used to insure continuous contact between the shaft and the slider rod. Finally the accelerometer pick up was mounted on the top of rod. The accelerometer was connected to the oscilloscope through a charger amplifier as shown in **Fig.3-c**.

The main task of the experimental work is to measure the forwarded and backward whirl frequencies. For this purpose, impact hammer test was used. In this test the rotor speed was assigned 0,200,400,600,800,1000 and 1200 RPM at clockwise and counterclockwise directions. For each speed an impact test was carried out. The time histories of the excited force and the response were recorded and analyzed by using SigView software package. The Fast Fourier Transformation (FFT) was performed from which the whirl frequencies were calculated.

#### 4. RESULTS AND DISCUSSIONS

Although the present analysis is hold for any number of discs and bearings, However, an example of a rotor consists of elastic shaft carrying three different size discs and supported by two identical bearings was considered for the numerical analysis. The journal bearings has the following specifications;  $D=0.019170$  m,  $L/d=1$ ,  $c=0.1454$ mm. The oil lubricant is SAE 20 with  $\mu =0.0562$  N.s/m<sup>2</sup>. For evaluating the bearing stiffness and damping, the value of Summerfield number was calculated from the above data and the graphs given by Lund, are employed. The numerical data of the model are listed in table .1

The validity and convergence of the present solution were checked by comparing with the ANSYS solution. MATLAB R2009 software was employed to solve Eq.(32) to evaluate the unbalance response. The number of modes of the present solution are varied from  $N=3$  to 6. For the two methods the discs are located at  $\zeta= 0.25, 0.5$  and  $0.75$ . The results of the two methods, as well as, the percentage errors are presented in **Table 2**. **Table 2** shows that, the present solution has better convergence at  $N=5$  where the percentage

error is not exceeded (5 %) .Hence using five modes is quite sufficient for the accurate analysis.

**Fig.4** shows the ANSYS simulation of the model. The unbalance response is displayed in figure. For the comparison purpose, the responses of the same model is plotted by using the present solution for  $N=3,4$  and 5 and shown in **Fig.4**. As it is clear from these figures, the results of the two methods are in a good agreement especially when  $N$  approaches 5.

To investigate the effect of spin speed on the forward and backward frequencies for the lowest three modes, Campbell diagram is plotted in **Fig.5**. This diagram is plotted by using the two methods, again. As it is clear from these figures, that, the agreements between the two solutions is good.

The main advantage of Campbell diagram is to test the stability and evaluate critical speeds of the rotor. In order to inspect stability; the values of the natural frequencies are checked at the selected range of spin speeds. When their values changed from real to complex the rotor is regarded unstable. The speeds causing such a change are referred as Threshold speeds. It is found that the present rotor model is always stable at the selected speed range.

The critical speeds can be evaluated from cambpell diagram by plotting a straight line with slope=1(the solid line in **Fig.5**). The points of intersections between this line and the frequencies curves give the critical speeds. Referring to **Fig.5** the critical speeds have the following values ; 630,660,780 and 1650 RPM. It is to be noted that, some of critical speeds cannot be detected from plotting the unbalance response curve since it consider the unbalance response for forward whirl speeds, only. Hence Campbell diagram is more effective tool in designing rotors since it is able to detect wide range of critical speeds.

The orbit plot response of the model as it spin at 960 RPM is shown in **Fig.6**. As one can see from the plot that, the larger orbit path is found under the location of heaviest disc.

For further investigation, the effect of disc locating and arranging, **Figs. 7,8 and 9** are created. In **Fig. 7** the discs are allow to locate close together by assigning  $\zeta=0.4,0.5$  and  $0.6$ . The unbalance response of this case is plotted. **Fig.7** indicates two information; firstly, the critical speeds decrease, secondly, one of critical speeds becomes insignificant (very small peak response). This means that as the discs spacing decreased



the multi rotor behavior approach that of the single rotor behavior.

The effect of discs arrangements are investigated in **Figs.8 and 9** .In **Fig.8** the discs are arranged in increasing size order, whilst ,in **Fig.9** in decreasing order . Comparing the response of the two cases indicates that; reverting the order of discs sizes gives a slight change in the critical speeds which may be ignored .This may be reasoned due to the dynamical symmetry of the supporting bearings which give nearly identical elastic curve.

The theoretical and experimental results of the two discs model is shown in **Fig.10**.In this figure the forward and backward whirl frequencies are shown .As it is clear that the results are in a good agreements where the maximum error is not exceeding 11%.The deviation between the two results may be attributed to the measuring error ,effect of internal damping and bearings in isotropic .

#### 4.CONCLUSIONS

In the present analysis, Galerkin method was used to evaluate the dynamical behavior of multi discs and bearing rotors. The present analysis can be used for any number of discs and bearings. All the rotor dynamic aspects; such as forward and backward whirl frequencies ,Campbell diagram ,stability, critical speed and unbalance response can be evaluated by using the present method .

The validity and convergence of the present analysis was performed by comparing with the Finite element solution and experimental results . The numerical results of a sample of three disc rotor showed that; the solution has better convergence when only five modes are employed, and the maximum error is not exceeded 5% .Hence the computation time and labor can be saved. The experimental results showed good agreements in measuring the forward and backward whirl frequencies with maximum error is not exceeding 11%. The effects of disc locations and arrangements are investigated .It is found that closing the space between the discs tends to decrease the critical speeds values and diminish some of them .So that the multi discs rotor behaves as a single rotor However reverting the location of the discs has insignificant effect on the critical speeds since it cause a slight change.

#### 5-REFERENCES

- A. G. Holmes, C. M. Ettles and I. W. Mayes, 1978, "*The Dynamics of Multi-Rotor Systems Supported on Oil Film Bearings*", J. Mech. Des., 100, 156 - 164.
- A.S. Das, J.K.Dutt, 2012,"*A Reduced Rotor Model Using Modified SEREP Approach for Vibration Control of Rotors, Mechanical Systems and Signal Processing*" 26,167–180.
- G. Genta, 2005,"*Dynamics Of Rotating Systems*", springer.
- J. Ding, 1997,"*Computation Of Multi-Plane Imbalance for a Multi-Bearing Rotor System*", Journal of Sound and Vibration 205 (3), 364–371.
- J. S. RAO ,1994,"*The Calculation of the Natural Frequencies of Multi-Disk-Rotor Systems Using the Influence Coefficient Method Including The Gyroscopic Effects*", Mech. Mach. Theory ( 29). pp. 739-748.
- J. W. Lund and K. K. Thomsen, 1978, "*A Calculation Method and Data for the Dynamic Coefficients of Oil-Lubricated*" Journal Bearings, Topics 'In Fluid Film Bearing And Rotor Bearing System Design And Optimization, ASME Design Engineering ,New York.
- L. Meirovitch, 1975, "*Elements Of Vibration Analysis*" Mcgraw-Hill, Inc.
- M. Geradin, N. Kill, 1984, "*A New Approach to Finite Element Modeling Of Flexible Rotors,*" Engineering Computations, 52–64.
- M. L. Adams &JR, 2010,"*Rotating Machinery Vibration, from Analysis to Troubleshooting*", CRC press, Taylor & Francis group, second edition.
- Q. Ding, A.Y.T. Leung, 2005 ,"*Experimental Study on Nonlinear Dynamic Behaviours of a Multi-Bearing Flexible Rotor System*", Journal of Vibration and Acoustics— Transactions of the ASME, 127, (4),408–415.
- R. D. Flack, R F. Lanes and P. S. Gambel, 1981,"*Effects Of Lubricant Viscosity on the*



*Experimental Response of a Three-Mass Flexible Rotor in Two Types of Journal Bearings ,Wear”, 67,201 – 216*

Xie Wenhua, Tang Youganga, Chen Yushub, 2008, “*Analysis of Motion Stability of the Flexible Rotor-Bearing System with Two Unbalanced Disks*”, Journal of Sound and Vibration 310, 381–393.

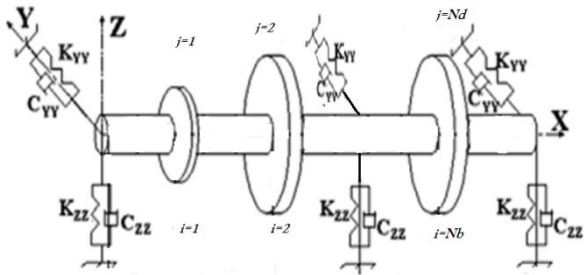


**Figure 1.** Multi discs and bearings model.

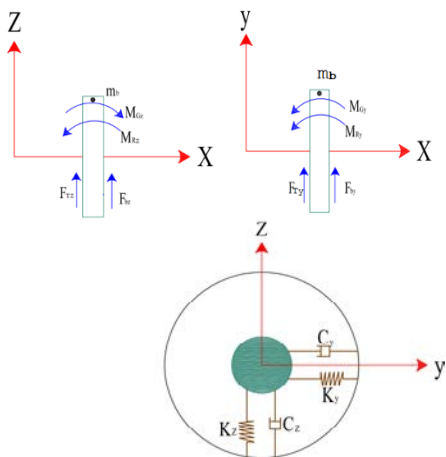


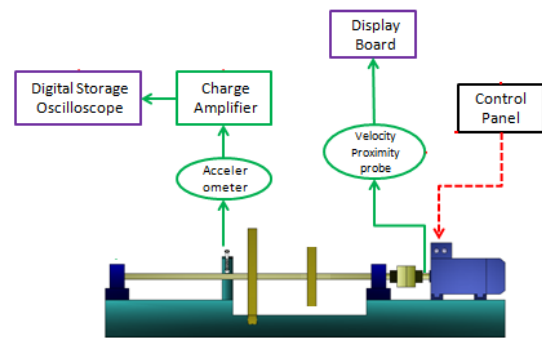
**Figure 2.** Disc and bearing modeling.



(a)



(b)



(c)

**Figure 3.** Experimental rig, instrumentations and connection block diagram.



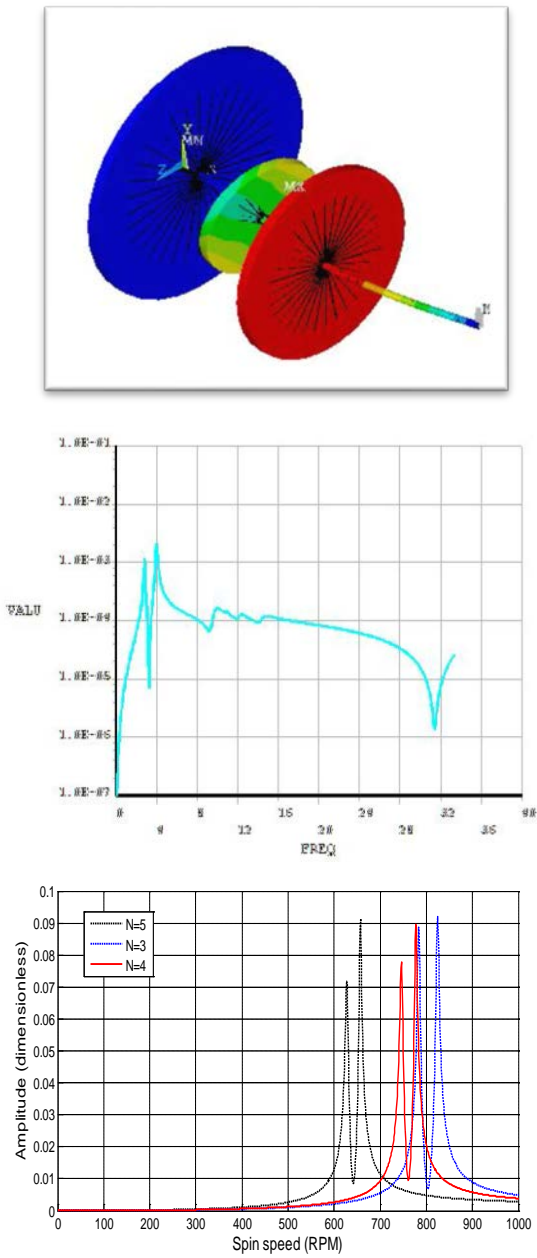


**Figure 4.** Model simulation , unbalance response by using ANSYS and the present method, for three discs rotor .

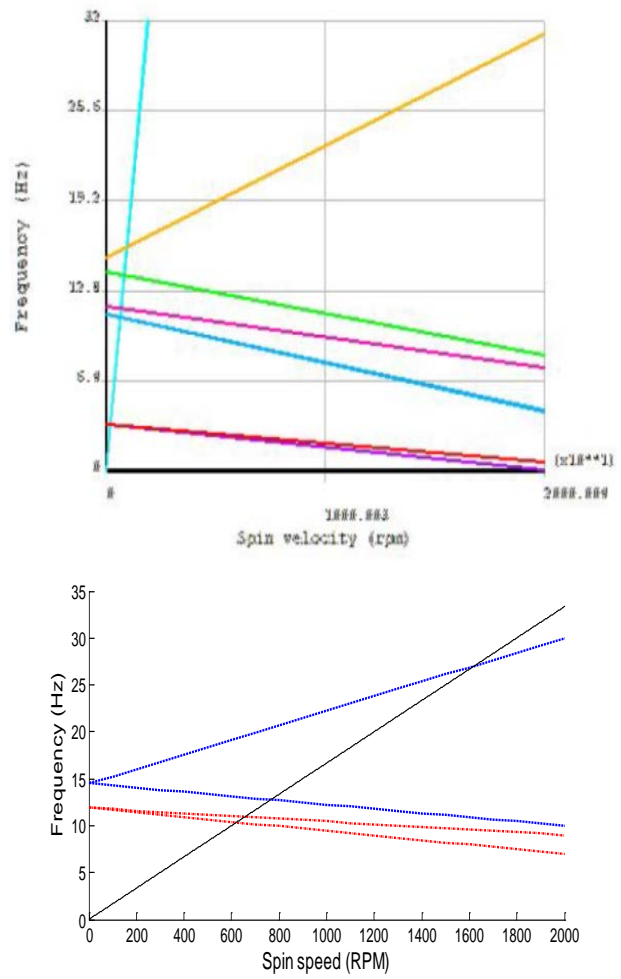


**Figure 5.** Campbell diagram , by ANSYS and the present method.

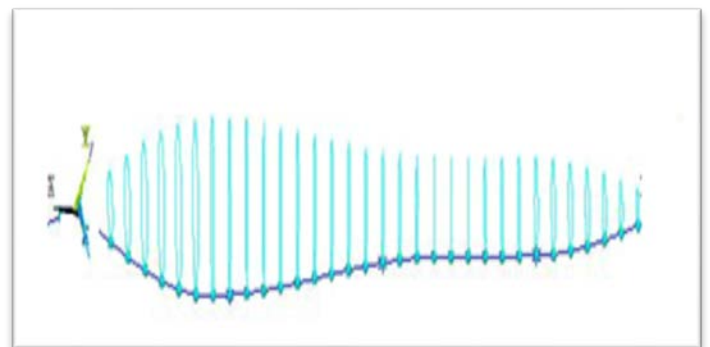


**Figure 5.** Orbit response of the three discs rotor spins at 960RPM.

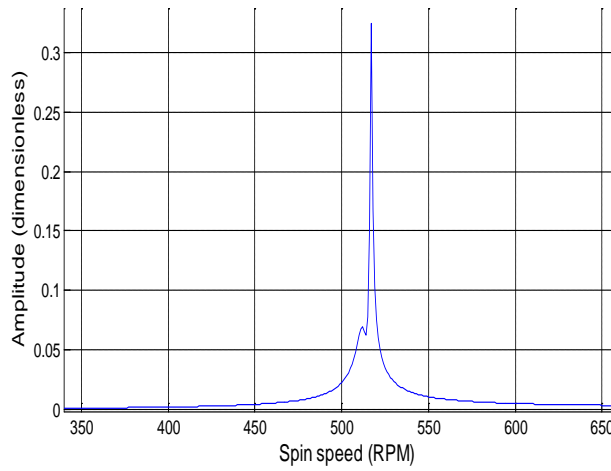
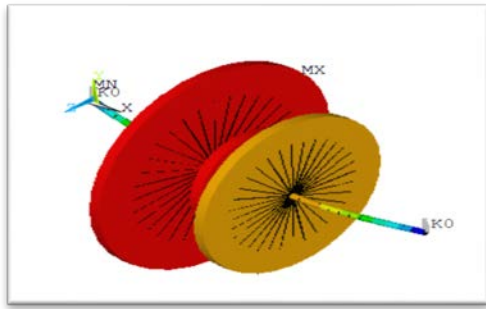


**Figure 7.** Model simulation and unbalance response for closing spaced discs case.

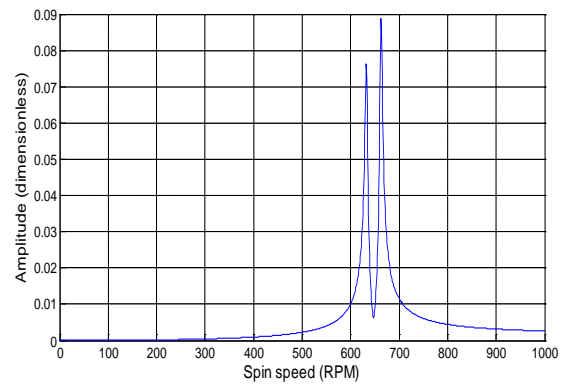
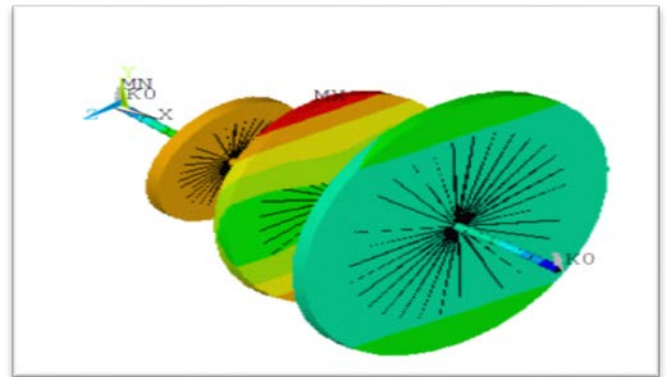


**Figure 8.** Model simulation and unbalance response of increasing order size discs case.

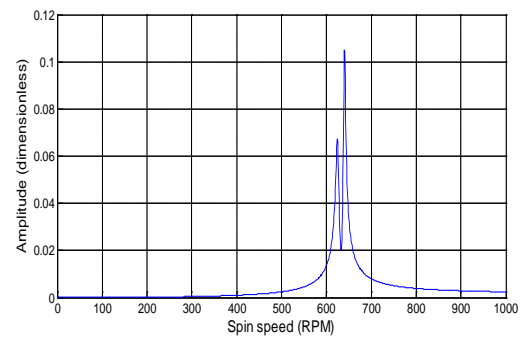
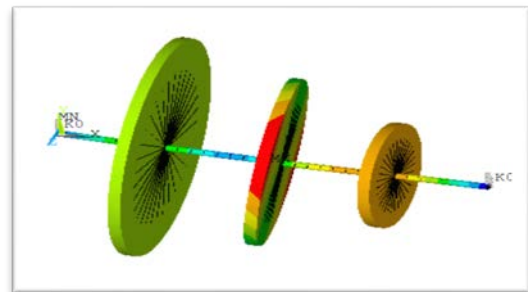


**Figure 9.** Model simulation and unbalance response of decreasing order size discs case.

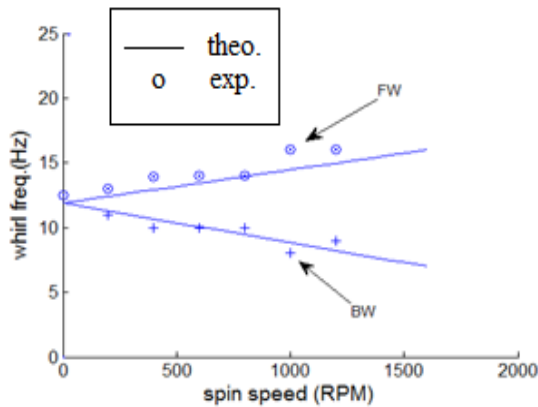


**Figure 10.** Theoretical and experimental whirl frequencies.

**Table 2.** Validity and convergence of the present.

S	Present solution							ANSYS	
	N=3	E%	N=4	E%	N=5	E%	N=6		E%
1	784	20.2	746	14.1	627	-3.8	623	-4.4	652
2	824	19.2	777	12.4	657	-4	653	-5.5	691

**Table 1.** Specifications of the theoretical and experimental models (in SI units).

<b>Bearing(1)</b> K <sub>xx1</sub> =17.249x10 <sup>6</sup> K <sub>yy1</sub> =1.294x10 <sup>6</sup> C <sub>zz1</sub> = 3.08x10 <sup>5</sup> C <sub>yy1</sub> = 2.05x10 <sup>4</sup>	<b>Bearing (2)</b> K <sub>xx</sub> =17.249x10 <sup>6</sup> K <sub>yy</sub> =1.294x10 <sup>6</sup> C <sub>zz</sub> = 3.08x10 <sup>5</sup> C <sub>yy</sub> = 2.05x10 <sup>4</sup>	<b>Disc(1)</b> d <sub>1</sub> =0.35 t <sub>1</sub> =0.013 ρ <sub>1</sub> =8205 m <sub>b</sub> =0.2 r=0.05
<b>Disc(2)</b> d <sub>2</sub> =0.167 t <sub>2</sub> =0.019 ρ <sub>2</sub> =8205 m <sub>b</sub> =0.2 r=0.05	<b>Disc(3)</b> d <sub>3</sub> =0.268 t <sub>3</sub> =0.02 ρ <sub>3</sub> =8205 m <sub>b</sub> =0.2 r=0.05	<b>Shaft</b> L <sub>s</sub> =1 d <sub>s</sub> =0.019 E=206x10 <sup>9</sup> ρ <sub>s</sub> =7800 damp=0.01

**NOMENCLATURE**

- A Shaft cross sectional area, m<sup>2</sup>
- C<sub>iz</sub> i<sup>th</sup> bearing damping coefficients, in z axis, N/m
- C<sub>iy</sub> i<sup>th</sup> bearing damping coefficients, in y axis, N/m
- c Bearing clearance, m
- D Bearing diameter, m
- ds Shaft diameter, m
- E Modulus of elasticity, N/m<sup>2</sup>
- r Disc eccentricity, m
- I Area second moment of inertia, m<sup>4</sup>
- F<sub>Zs</sub> Spring forces at z axis, N
- F<sub>ys</sub> Spring forces at y axis, N
- F<sub>zD</sub> Damping forces at z axis, N
- F<sub>zI</sub> Damping forces at y axis, N
- F<sub>zIb</sub> Imbalance forces at z, y axis, N

- M<sub>zG</sub> Gyroscopic moments at z, y axis, N.m
- M<sub>zb</sub> Inertial moments at z, y axis, N.m
- I<sub>p</sub> Polar moment of inertia, Kg.m<sup>2</sup>
- I<sub>T</sub> Transverse moment of inertia, kg.m<sup>2</sup>
- K<sub>zi</sub> i<sup>th</sup> bearing stiffness, in z axis, N/m
- K<sub>yi</sub> i<sup>th</sup> stiffness, in y axis, N/m
- L Bearing length, m
- Ls Shaft span length, m
- m<sub>d</sub> Disc mass, kg
- N Mode number or RPM
- p or p(t) Generalized coordinate at y axis
- μ, η Dimensionless coordinates at z and y axis
- λ Eigen values of free-free beams
- φ, Φ

$\zeta$	Dimensionless lateral coordinate
$\rho$	Density, $kg/m^3$
$\mu$	Oil viscosity, $Pa\cdot sec$
$\tau$	Dimensionless time
$\Omega$	Disc spin speed, r/s
$\omega$	Natural frequency, r/s

**Elements of [A] and [B] ;**

$$a_{s,r} = \int_0^1 \phi_s^{IV}(\zeta) \phi_r(\zeta) d\zeta = \int_0^1 \varphi_s^{IV}(\zeta) \varphi_r(\zeta) d\zeta ,$$

$$a_{s,1+N} = \int_0^1 \phi_s^{IV}(\zeta) d\zeta = \int_0^1 \varphi_s^{IV}(\zeta) d\zeta$$

$$a_{s,2+N} = \int_0^1 \zeta \phi_s^{IV}(\zeta) d\zeta = \int_0^1 \zeta \varphi_s^{IV}(\zeta) d\zeta ,$$

$$b_{s,r} = \int_0^1 \phi_s(\zeta) \phi_r(\zeta) d\zeta = \int_0^1 \varphi_s(\zeta) \varphi_r(\zeta) d\zeta$$

$$b_{1+N,r} = \int_0^1 \phi_r(\zeta) d\zeta = \int_0^1 \varphi_r(\zeta) d\zeta ,$$

$$b_{2+N,r} = \int_0^1 \zeta \phi_r(\zeta) d\zeta = \int_0^1 \zeta \varphi_r(\zeta) d\zeta$$

$$b_{s,1+N} = \int_0^1 \phi_s(\zeta) d\zeta = \int_0^1 \varphi_s(\zeta) d\zeta ,$$

$$b_{1+N,1+N} = \int_0^1 (1) d\zeta = \int_0^1 (1) d\zeta = 1 ,$$

$$b_{2+N,1+N} = b_{1+N,2+N} = \int_0^1 \zeta .d\zeta = 1/2 ,$$

$$b_{s,2+N} = \int_0^1 \phi_s(\zeta) .\zeta .d\zeta = \int_0^1 \varphi_s(\zeta) .\zeta .d\zeta$$

$$b_{2+N,2+N} = \int_0^1 \zeta^2 .d\zeta = 1/3$$

**Elements of matrix H, L, T, V and W;**

$$h_{s,r} = \phi_r(\zeta_1) \phi_s(\zeta_1) = \varphi_r(\zeta_1) \varphi_s(\zeta_1)$$

$$h_{1+N,r} = h_{s,1+N} = \phi_s(\zeta_1) = \varphi_s(\zeta_1)$$

$$h_{1+N,1+N} = 1$$

$$h_{2+N,r} = h_{2+N,1+N} = h_{2+N,r} = h_{2+N,1+N} = h_{2+N,2+N} = 0$$

$$l_{s,r} = \phi_r(\zeta_3) \phi_s(\zeta_3) = \varphi_r(\zeta_3) \varphi_s(\zeta_3)$$

$$l_{1+N,r} = l_{s,1+N} = \phi_s(\zeta_3) = \varphi_s(\zeta_3)$$

$$l_{1+N,1+N} = 1$$

$$l_{2+N,r} = l_{2+N,1+N} = l_{2+N,r} = l_{2+N,1+N} = l_{2+N,2+N} = 0$$

$$t_{s,r} = \phi_r(\zeta_2) \phi_s(\zeta_2) = \varphi_r(\zeta_2) \varphi_s(\zeta_2) ,$$

$$t_{1+N,r} = t_{s,1+N} = \phi_s(\zeta_2) = \varphi_s(\zeta_2) , \quad t_{1+N,1+N} = 1$$

$$t_{2+N,r} = t_{2+N,1+N} = t_{2+N,r} = t_{2+N,1+N} = t_{2+N,2+N} = 0$$

$$v_{s,r} = \phi_r'(\zeta_2) \phi_s'(\zeta_2) = \varphi_r'(\zeta_2) \varphi_s'(\zeta_2)$$

$$v_{s,1+N} = v_{s,2+N} = v_{1+N,r} = v_{1+N,1+N} = v_{1+N,2+N} = v_{2+N,r} = v_{2+N,1+N} = v_{2+N,2+N} = 0$$

$$w_{l,s} = \phi_r(\zeta_2) , \quad w_{l,1} = 1 , \quad w_{l,2} = \zeta_2$$